Pergamon

Geochimica et Cosmochimica Acta, Vol. 65, No. 16, pp. 2641–2649, 2001

0016-7037/01 $20.00 + .00

PII S0016-7037(00)00624-X

The proximity effect on semiconducting mineral surfaces: A new aspect of mineral surface reactivity and surface complexation theory?

UDO BECKER,[1] KEVIN M. ROSSO,[2] and MICHAEL F. HOCHELLA, JR.[3]

[1]Institut für Mineralogie, Universität Münster, Corrensstraβe 24, D-48149 Münster, Germany
[2]W.R. Wiley Environmental Molecular Sciences Laboratory, Pacific Northwest National Laboratory, P.O. Box 999, K8-96, Richland, WA 99352, USA
[3]Department of Geological Sciences, Virginia Polytechnic Institute and State University, Blacksburg, VA24061, USA

(*Received July* 19, 2000; *accepted in revised form March* 19, 2001)

Abstract—The observation and description of surface proximity effects, whereby the chemical reaction of one surface site influences the electronic structure and reactivity of neighboring or nearby sites, is presented in this study for the semiconducting minerals galena (PbS) and pyrite (FeS_2). The methods used to study this effect include *ab initio* molecular orbital calculations and scanning tunneling microscopy and spectroscopy. The surface proximity effect can be manifested in different ways, although the principle is the same. For example, we predict that electron transfer in redox reactions on galena surfaces can involve separated sites with specific and special locations. Another example is seen for pyrite where the oxidation of one site on a terrace influences next-nearest neighbor sites, making them far more susceptible to oxidative attack relative to sites further away. The range of potential applications of the surface proximity effect model is also outlined for a number of environmentally and industrially important examples. These findings, in combination with surface complexation theory, an important model for attachment/detachment reactions at mineral–water interfaces, may eventually lead to an extended model that will include the specific influence of semiconductor-type proximity effects. *Copyright © 2001 Elsevier Science Ltd*

1. INTRODUCTION

Surface complexation theory has been one of the most powerful tools to describe the reactivity of mineral surfaces (e.g., Hingston, 1981; James and Parks, 1982; Barrow, 1987; Davis and Kent, 1990; Dzombak and Morel, 1990; Stumm, 1992; Hiemstra and Van Riemsdijk, 1999). In the most basic form of such an approach, the reactivity is described as that of individual and independent site types at the surface (often at a particular pH) for a species in solution or air. Thus, to derive reactivities of mineral surfaces from such an approach, one would ideally want to evaluate the number of sites on terraces, steps, and kinks and multiply each with its respective equilibrium constant or, for kinetic information, rate constant. Typically, as a result of the lack of information of the exact distribution of different surface sites and their individual reactivities, an equilibrium constant for the most reactive site or an average constant is applied. This approach has been successful on many, mostly insulating, mineral surfaces. For example, the rates for silicate dissolution (e.g., Drever and Stillings, 1997; Poulson et al., 1997; Koretsky et al., 1998; Rufe and Hochella, 1999), sulfate growth and dissolution (Bosbach et al., 1998; Pina et al., 1998; Kubota et al., 2000; Srinivasan et al., 2000), cation exchange reactions (e.g., Kraepiel et al., 1999), and adsorption reactions have been adequately described in this way.

Site–site interactions in surface complexation theory have been empirically taken into account by applying, e.g., the Frumkin-Fowler-Guggenheim (FFG) adsorption isotherm. In this approach, the Langmuir isotherm [$\theta/(1-\theta)$ with θ being the quotient of the concentration adsorbed to the surface and the total concentration of the species] is multiplied by an additional factor $\exp(-2a\theta)$. In the FFG approach, a is a constant that describes the extent of lateral interactions. By use of this type of isotherm, Ardizzone et al. (1998) have quantified the pyridine–aniline interactions on different mineral surfaces. Other examples of analyzing site–site interactions that use the FFG equation are the flotation mechanisms of quartz in the presence of alkylammonium salts (Montes et al., 2000), the Ag-Ag interaction during silver adsorption on the Si (111) surface (Müller et al., 1994), and attractive interactions between Ca^{2+} ions on kink sites with impurities (heavy metals or phosphate; Svensson and Dreybrodt, 1992). In many of these examples, sorbate–sorbate interaction is assumed to take place directly between the sorbed surface species, e.g., by electrostatic repulsion or attraction.

However, for many adsorption reactions and redox processes in nature and in technical processes involving mineral surfaces, the electronic properties of semiconducting minerals introduce the possibility for unique behavior, such as the coupling of spatially separated redox species by electron transfer through near surface layers. Naturally occurring and relatively abundant semiconducting materials, minerals such as hematite (Fe_2O_3), pyrite (FeS_2), and galena (PbS), are some of the most important phases near the Earth's surface. Hematite influences transition metal mobility in many soils (Cornell and Schwertmann, 1996), and pyrite (Jambor and Blowes, 1994) and galena (Rimstidt et al., 1994) often act as key components in acid mine runoff. Reactions that occur on the surfaces of these minerals largely dictate the properties and importance that they display in nature, reactions that have for years been modeled by means of various interpretations of surface complexation theory.

To understand the characteristic reaction mechanisms on semiconducting surfaces, it is crucial to understand the electronic structure of these surfaces or of specific sites thereon. Because of the narrow band gap of semiconductors, the elec-

*Author to whom correspondence should be addressed.

tronic structure plays a key role in determining if electron transfer from or to a surface site can take place. This is not only dependent on the local density of filled states in the uppermost 2 to 3 eV of the valence band (for oxidation reactions) or on the conduction band (for reduction reactions), but also on electronic properties such as the orbital symmetry (Nilsson et al., 1997; Gokhale et al., 1998; Fohlisch et al., 2000; Pascual et al., 2000) or the spin configuration (Becker and Hochella, 1996). In addition, because of the high degree of delocalization of electronic states in the bulk and surfaces of these minerals (Becker et al., 1997b; Rosso et al., 1999a), the electronic properties of one particular site are often easily perturbed by physical and chemical processes that occur some distance away. In this respect, it may be helpful to understand the various ways that semiconducting surfaces and solids can be modified by external and internal influences. It is well known that the reactivity of sulfide surfaces is highly dependent on the electrochemical potential that is applied to them. This can play an important role in technical processes such as flotation (Prestidge et al., 1993; Tao et al., 1994) and in the form of cyclic voltametry in the analysis of redox reactions of sulfide surfaces (Cisneros-Gonzalez et al., 1999; Lin and Say, 1999). In addition, the local electronic structure (in the form of so-called band bending; Suganuma and Tomitori, 2000), and thus the reactivity of a surface site, can be significantly changed when a tip of a scanning tunneling microscope approaches a surface (Hamers et al., 1996; Higgins and Hamers, 1996). Similar electronic processes occur if a charged or polarizing species approaches a surface site. The adsorption of polarizing species, even at low concentrations, can modify the electrostatic potential distribution at the surface-liquid interface. The so-called Helmholtz layer can therefore change the electronic structure at the interface and alter the reactivity in the near surface region (Albery et al., 1996; Natarajan et al., 1998).

In addition to externally applied fields or perturbations that cause major changes in the electronic structure of semiconductor surfaces, and to a lesser extent the bulk electronic structure, there can be internal effects that alter the electronic and reactive properties of these solids. The most common example is probably the effect of impurities and defects, which often act in a similar way as dopants in technically applied semiconductors. These can be substitute ions, interstitial ions or atoms, or vacancies. In some cases, the concentrations of the respective impurity can be very low, and thus the average distances between impurity sites can be more than several tens of ångstroms. Nevertheless, these minor amounts of impurities can control whether a mineral is an *n*-type or *p*-type semiconductor and thus the facility of reduction or oxidation reactions (Ellmer and Hopfner, 1997; Oertel et al., 1999). This is even more noteworthy because the nearest, e.g., substitute atoms can be several bond distances away from the actual redox reaction site.

Keeping all these examples in mind, the next obvious step to consider is to have dopantlike atoms or molecules sorbed to the surface. This means that different species on the surface that are not bonded to each other can interact by influencing the electronic structure of the surface in the vicinity of their respective adsorption sites. In this context, the surface can either be part of the overall reaction (that is, the oxidation states of species in the mineral surface change) or the surface plays the role of a catalyst by allowing charge transfer to take place between the two reactants on the surface. Such catalytic charge transfer reactions are known for some industrial and naturally occurring surfaces (Maldonado-Hodar et al., 1996; Tessis et al., 1999; Herrmann and Disdier, 2000).

In this study, we have gathered direct microscopic and spectroscopic evidence and supporting theoretical evidence for what we call the surface proximity effect, whereby the chemical reaction of one surface site influences the electronic structure and reactivity of neighboring or nearby sites by means of electron transfer through the near surface layers. We believe the surface proximity effect to be central in describing surface chemistry on all semiconducting minerals. With the advent of the scanning tunneling microscope (STM), it has become possible to investigate the electronic structure and characteristics of semiconducting surfaces with atomic resolution (Murray et al., 1994; Becker et al., 1997a; Eggleston, 1999; Rosso and Hochella, 1999). Recently, we have investigated hematite, pyrite, and galena surfaces by use of STM, scanning tunneling spectroscopy (STS), and *ab initio* molecular orbital calculations. The latter, in part, were specifically designed to help interpret STM-STS results (Becker and Hochella, 1996; Becker et al., 1996, 1997a,b; Rosso et al., 1999a,b). In this study, we extend these studies to the point needed to identify and begin to quantify the surface proximity effect. Even though we propose mechanisms for how separated species may interact via the semiconducting substrate from the spectroscopic, microscopic, and quantum mechanical evidence that we gathered, these can only serve as an additional approach to interpret macroscopic adsorption experiments without making the latter ones obsolete. This is because to this point, it is very difficult to derive, e.g., pH-dependent macroscopic adsorption isotherms from microscopic data at the molecular scale.

Two example cases of proximity effects will be discussed. The first example involves the oxidation of galena via interaction with ferric iron and water. In this case, Fe^{3+} acts as the oxidizing agent (electron acceptor); water promotes this reaction and supplies the oxygen necessary to produce sulfate as illustrated in the overall reaction (Rimstidt et al., 1994):

$$PbS + 8\,Fe^{3+} + 4\,H_2O \leftrightarrow Pb^{2+} + SO_4^{2-} + 8\,H^+ + 8\,Fe^{2+} \quad (1)$$

However, we will show that the ferric iron and the water molecule do not have to be bonded to the same surface atom. The second example deals with the attack of molecular oxygen and water on the surface of pyrite. In these examples, we have spectroscopic and quantum mechanical evidence of various aspects of proximity effects.

2. MATERIALS AND METHODS

All calculations on galena were performed on a $4 \times 4 \times 2$-atom PbS cluster (16 Pb and 16 S atoms) by means of a hybrid method of the Hartree-Fock (HF) and Becke3-DFT (density functional theory; Fig. 1a) approach incorporated in the computer program package Gaussian98 (Frisch et al., 1998). Hay and Wadt–type pseudopotentials have been applied for Pb and S with a double ζ valence basis set. The use of a cluster of this size was the best choice because the theoretical part of this study was designed to answer a number of questions. First, we wanted to find out if two or more species can influence each other even if they are adsorbed to two different

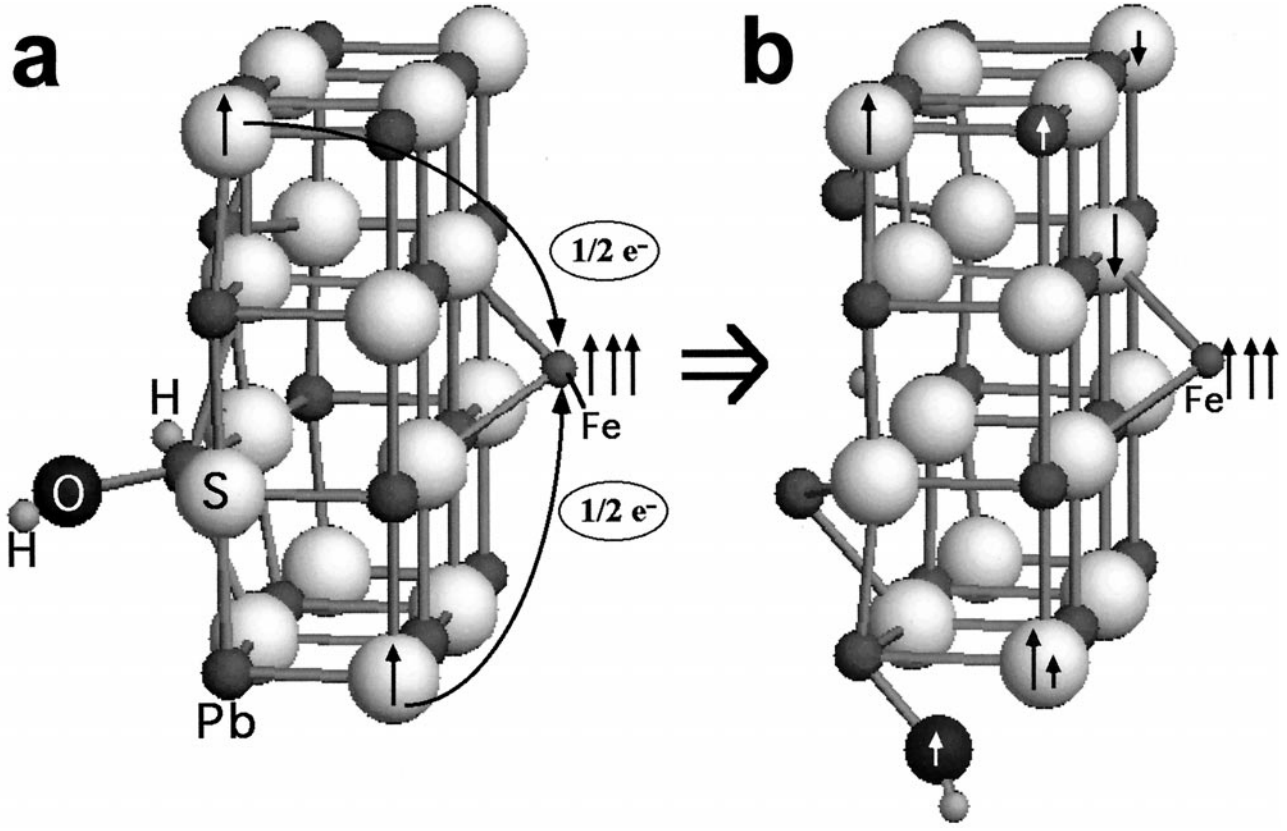

Fig. 1. Slightly tilted side views of a galena cluster with ferric iron and dissociated water adsorbed. (a) Starting position from where OH^- and H^+ were allowed to move and the cluster to respond to the interaction of water and ferric iron. Unpaired spins on S and Fe are designated with ↑ and the "pathway" of electron transfer is indicated by curved arrows. Minor electron transfer (<0.1 e^- per atom) also takes place from all the other sulfur atoms to the ferric iron. (b) Final atomic and spin configuration due to the remote interaction of Fe and OH^-.

sides of a slab—or, in terms of the model shown in Figure 2, if they are adsorbed on both sides of a double step on a surface. This computational setup allows one to study which site types—i.e., kink sites, step edges, and terracelike sites—undergo the most significant electronic structure changes during reaction. As shown by Becker et al. (1997c), the edge effects penetrate such a cluster by only 2 to 3 Å, and the inner atoms at the surface of the cluster are a good representation of the electronic structure and the chemical behavior of terraces. In addition to the evaluation of electronic structure changes during reactions, the cluster approach allows one to study if the adsorption sites of two independent adsorbing species are different from the combined adsorption. If a difference is found to exist, one can evaluate if charge transfer through the near surface layers that was induced by one adsorbing species leads to the mobilization of another species or to other reactions such as dissociation.

The experimental and theoretical methods for obtaining STM images and STS spectra of pyrite surfaces and for calculating electronic properties and reaction paths are described in Rosso et al. (1999a,b).

3. RESULTS

The starting (independent reaction of PbS with H_2O and Fe^{3+}) and ending (combined attack) simulated clusters are shown in Figure 1. In Figure 1a, Fe^{3+} has been attached and geometry optimized on one side of the cluster, and the H_2O has been dissociated (which is energetically more favorable than the undissociated case) and independently optimized on the other side of the cluster. The $(OH)^-$ and the H^+ find local energy minima in positions above a lead and a sulfur atom, respectively, in the middle of the galena cluster surface. The energetically most favorable spin configuration of this setup is an $S = 0$ system (all orbitals fully occupied).

When the Fe^{3+} (five unpaired spins, $S = 5/2$) approaches the cluster, spin density transfer takes place from the Fe^{3+} to the galena cluster and electron density transfers in the opposite direction. With dissociated water attached to the relaxed surface on the opposite side of the cluster (still in the position before the ferric ion was attached), sulfur atoms at opposite ends of one cluster side become spin polarized ($S = 1/2$, marked with ↑ Fig. 1a), and three unpaired spins remain with the iron atom. This spin configuration [i.e., S(Fe) = 3/2 and S(cluster) = 2/2 → S_{tot} = 5/2] is more energetically favorable than any other according to the hybrid Hartree-Fock/Density Functional Theory (HF-DFT) approach. We have tested the most energetically favorable spin configuration by comparing the energies of different total spin settings (S_{tot} = 1/2, 3/2, 5/2, and 7/2) for the initial (Fig. 1a) and final (Fig. 1b) positions and three intermediate positions of the hydroxide ion along its

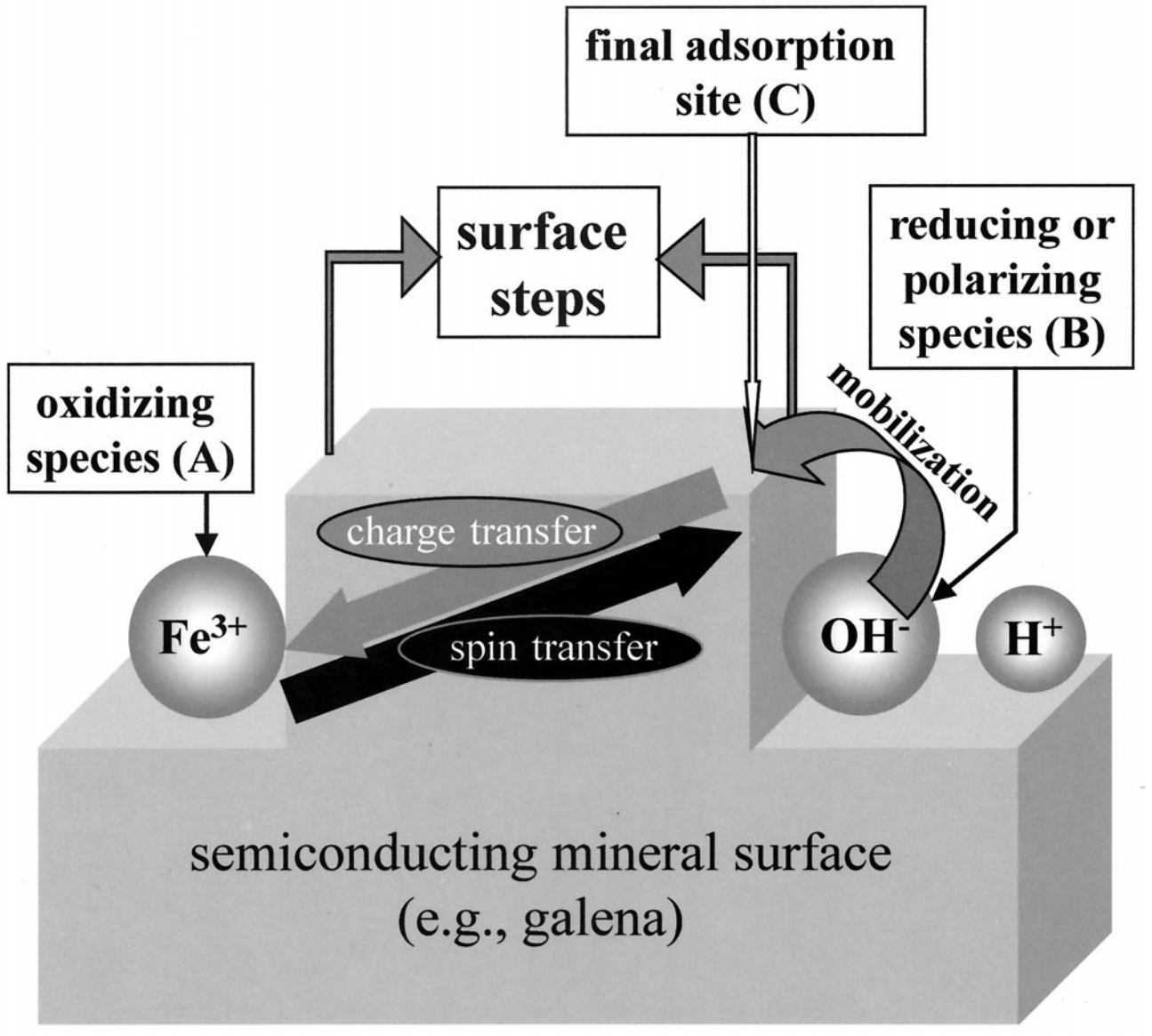

Fig. 2. An example model of the proximity effect on semiconducting mineral surfaces. Species A is an electron acceptor (oxidizing species). The electron may come from a reducing mineral surface or a reducing species B. In the latter case, charge density or electrons are transported through the mineral surface layers or along specific pathways, e.g., along steps. Because of the interdependent reactions of A and B, one of the species can get mobilized and adsorb to the final adsorption site C.

pathway shown in Figure 1. Even though Fe(III, $S = 5/2$) is a much more stable species than Fe(III, $S = 3/2$) as a free ion or in solution, when in contact with a reducing surface, it moves electronically toward a Fe(II)-like species. Therefore, it becomes understandable why the Mulliken population density analysis indicates a S(Fe) = 3/2 configuration.

However, the adsorbed Fe can also not be described as a Fe(II) ion yet that would have a spin of 4/2 or 0. This is another example of why species in contact with the delocalized electronic system of a semiconductor cannot be treated as entities stuck together with the same local electronic properties as their respective free ions. The electron transfer mainly occurs from the spin-polarized sulfur atoms through the cluster to the iron atom and surprisingly *not* from the sulfur atoms that are bonded to the ferric iron. As a result of the charge transfer and the spin polarization of the cluster corners, the hydroxyl group becomes mobilized and moves toward and around the closest corner that is spin polarized (Fig. 1b). It should be noted that the whole path is energetically downhill, with no local energy minima along the way, as in the case where there is no Fe attached on the other side of the cluster. Finally, the hydroxyl group finds its energy optimum at an almost equidistant position to a sulfur and a lead atom (Pb-O = 2.02 Å, S-O = 2.28 Å). The S-O distance is significantly longer than the S-O bond length in a sulfate ion (1.43 Å) but much shorter than the shortest S-O distance without the influence of ferric iron (4.5 Å). Surprisingly, the Pb-O bond length is shorter than in litharge (Pb-O, 2.33 Å, Moore and Pauling, 1941). Another striking feature is

the response of the Pb atoms on the surface to the oxidation by ferric iron and the mobilization of hydroxyl. The two center Pb atoms on the water side of the cluster shift positions enough to break three of the original five bonds to sulfur atoms present in the original cluster. This is consistent with the release of lead from the surface during oxidation reactions that has been experimentally observed in several previous studies (Buckley and Woods, 1984; Kim et al., 1994). During the mobilization of the OH^- group, the spin distribution in the cluster changes significantly and is indicated by $\uparrow$ and $\downarrow$ in Figure 1b (shorter $\uparrow$ and $\downarrow$ are used for fractions of spin density units).

The proximity effect suggested here indicates that sorbed species (e.g., species A in Fig. 2) may modify sites in special positions such as corners of a cluster (comparable with kink sites on a surface; site C in Fig. 2) even though they are not in the immediate vicinity of the initial reaction. In addition, an equilibrium position of a surface species (original position of species B in Fig. 2) may be modified by another species several nanometers away and only acting via changes in the electronic structure of the near surface region such that the first surface complex gets mobilized. Finally, this surface complex may find a new energetic minimum at the surface that can be located at a prominent surface feature such as a kink site or corner site (site C), which does not have to be in the direct neighborhood of the first adsorption site or bonded to the second species.

Although the calculations presented above strongly suggest the importance of proximity effects, their direct observation with STM-STS is clearly desirable. We have found strong evidence of this in STM images of oxidizing pyrite via O_2 in vacuum. Figure 3a shows a typical low negative bias STM image of a pristine pyrite (100) surface, exposed by in-vacuum fracture. Images taken at low positive biases give the same image, indicating that both the highest occupied and lowest unoccupied states are contributed from atoms at the same position on the surface. The image shows an array of single bright spots, representing areas of high tunneling current, which match the expected positions of Fe atoms on this surface. The sulfur dimers between the iron positions are not visible. The correlation between the bright spots in the STM image and surface iron atoms is substantiated by molecular orbital calculations that indicate that the highest occupied state (the top of the valence band) at the (100) surface of pyrite is mostly Fe $3d_z2$ in character, and the lowest unoccupied state (the bottom of the conduction band) is of mixed Fe $3d_z2$ and S $3p$ character (Rosso et al., 1999a). In fact, experimental tunneling spectra observed above individual atomic positions on the pyrite surface (Fig. 3b) are consistent with calculated tunneling spectra derived from tip positions over Fe and S_2 surface sites (Fig. 3c). Therefore, we are confident that the bright spots in Figure 3a not only represent iron frontier orbital contributions projecting into the vacuum from the surface, but that the tunneling current (the brightness of the spots in plane view or the height of the spots in oblique view) is proportional to the local density of states at each individual iron site on the surface.

When controlled oxidation experiments are conducted in vacuum, area-averaged STS spectra show a progressive decrease in state density of the highest occupied and lowest unoccupied states as exposure to O_2 is increased (Rosso et al., 1999b). Consistent with this, ultraviolet photoelectron spectroscopy (UPS) observations show a flattening of the top of the

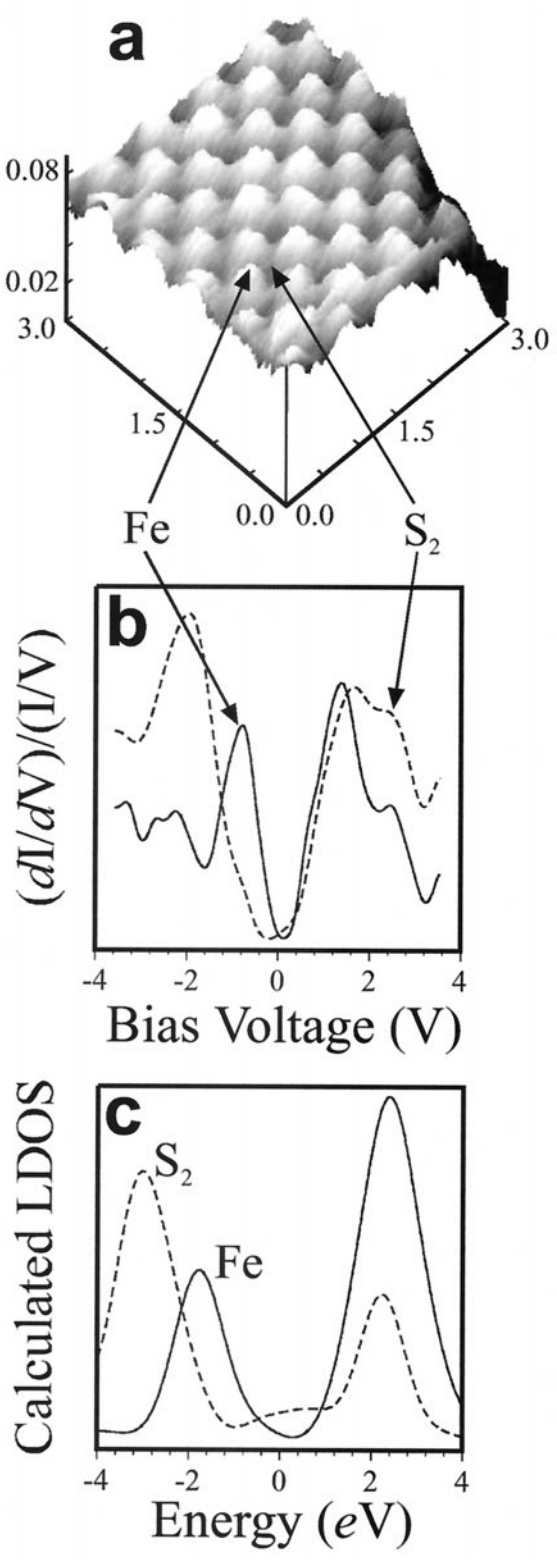

Fig. 3. (a) Atomic-scale topographic ultrahigh vacuum (UHV) STM image of in-vacuum cleaved pyrite (100). The image is as collected (i.e., not filtered). The tunneling conditions were −0.2 V bias and 2 nÅ set point current. All scale bars are in nanometers. (b) Single-point normalized (dI/dV)/(I/V) tunneling spectra collected on a pristine pyrite surface as shown. (c) Calculated local densities of states (LDOS) for tip positions over surface S_2 and Fe sites on (100) pyrite.

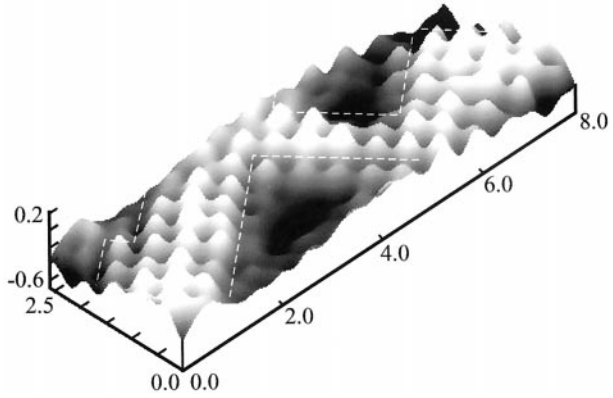

Fig. 4. Current UHV STM image of pyrite (100) surface exposed to 4 langmuirs oxygen (equivalent to an exposure of 10^{-6} torr oxygen for 4 s). Tunneling conditions: −20 mV bias, 3 nÅ set point current in constant height mode with the tip scanning from left to right along the long axis of the image. The oxidized patches are the low black areas. White dashed lines denote the boundary between unoxidized Fe sites affected by neighboring oxidized sites and the still unaffected regions. This image was band-pass Fast-Fourier transformed (FFT) filtered to remove high-frequency noise. Scale bars are in nanometers.

valence band with increased oxidation (Eggleston et al., 1996; Rosso et al., 1999b). As expected from the interpretation of the STM images of the unoxidized surface and the area-averaged STS and UPS spectra during oxidation, the bright spots in the STM images are "quenched" during oxidation. As has been observed before in ambient STM images of air-oxidized pyrite (Eggleston et al., 1996), surface irons do not react with O_2 randomly, but discrete patches of oxidation develop. These patches are typically bounded by rows of iron atoms along the surface cell diagonal—that is, the [11] direction.

The most intriguing part of the pyrite oxidation process, resulting in the discovery of another proximity effect, is the detail in the STM images taken in vacuum during oxidation. In all of the highest-quality images, the oxidized patches do not have sharp edges. Instead, bordering the patches are always spots that are not as high (intense) as the spots two or more iron atoms away from the oxidized patch, as shown in Figure 4. This STM image was collected in constant-height mode (relatively low feedback gains, high scan rate), which means that the tip was rastered in a flat plane parallel to the surface. Tunneling current differences from site to site are therefore captured in the error signal image (current image as shown in Fig. 4), whereas the apparent height image (topographic image) remains featureless (<0.1 Å maximum relief in this case). As the tip passes over an oxidized area, the decrease in the local density of states at Fe sites causes the measured tunneling current to decrease, making the area seem dark in the image. This decrease is found to be gradual from unoxidized to oxidized sites, occurring over a distance of almost 8 Å. Analysis of the image data strongly suggests that local state density is being withdrawn from at least near the Fermi level of iron atoms bordering an oxidized patch. It is possible that this reduction in tunneling current along the borders of the patches could be due to a decrease in the tunneling transmission probability because of an increase in the work function of the pyrite surface as it oxidizes. Sorption of species on pyrite can do this, as was shown by the adsorption of Br_2 on in-vacuum cleaved pyrite (Pettenkofer et al., 1991).

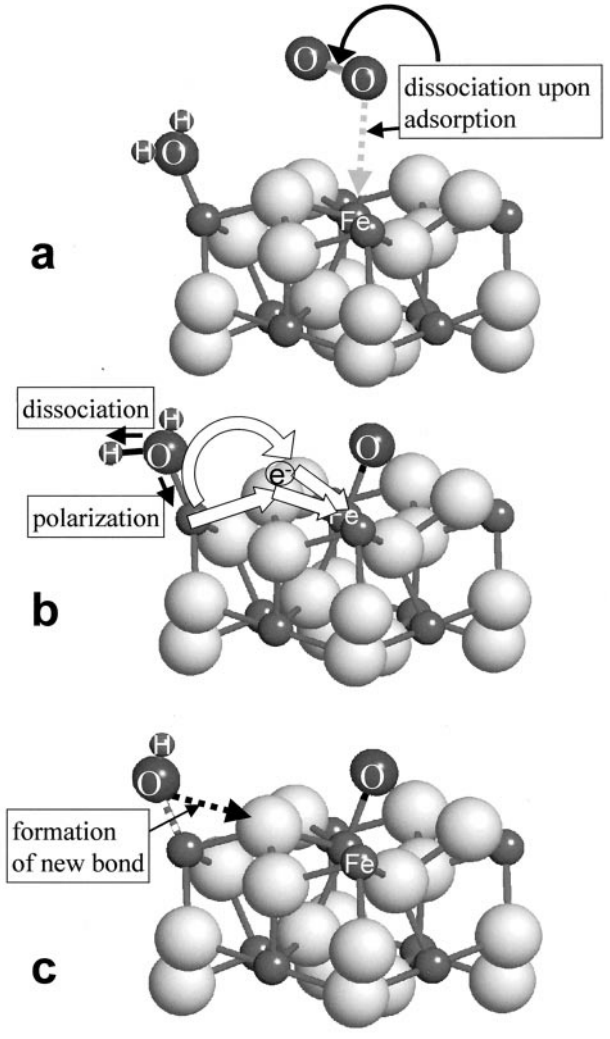

Fig. 5. (a) Illustration of the oxidation of pyrite (100) by coadsorption of O_2 and H_2O. In the absence of O_2, H_2O is weakly bound to the surface and does not dissociate. (b) O_2 dissociatively chemisorbs to Fe sites on the surface, leaving Fe-O groups; draws electron density from surrounding sites; and causes sorbed H_2O to dissociate. (c) Product hydroxyls are able to mount a nucleophilic attack on partially electron-depleted S atoms.

However, no significant work function change was noted in this study with UPS as pristine pyrite was progressively oxidized under controlled conditions in vacuum. Therefore, Figure 4 (and many other images like this) seems to hold direct evidence that O_2, in this case reacting with a surface Fe atom on pyrite, also perturbs the next nearest surface Fe atom (at a distance of nearly 4Å) through shared surface sulfur dimers. It is also likely that this perturbation makes these bordering Fe atoms more susceptible to electrophilic attack, as the oxidation process proceeds by enlarging existing patches, not starting new ones.

Proximity effects can explain why the combined attack of H_2O and O_2 enhances the oxidation rate of pyrite as compared with molecular oxygen by itself (see Fig. 5 and also Guevremont et al., 1998; Rosso et al., 1999b). O_2 interacts strongly with surface Fe sites and has a tendency to dissociate, forming Fe-O groups across the surface. Consistent with the STM

observations described above, sorbed O is predicted to pull electron density from underlying and surrounding Fe and S surface atoms nearby the adsorption site. When H_2O molecules alone sorb to the pyrite surface, they weakly bind to Fe sites and show no tendency to dissociate into hydroxyls and protons (Fig. 5a). But when surface Fe-O groups are present (i.e., coadsorption with O_2), H_2O interacts more strongly with available Fe sites adjacent to Fe-O groups (Fig. 5b, c). This occurs because the partial loss of electron density at these sites increases their affinity for the lone pair electrons on H_2O molecules. In this case, H_2O dissociation is favored, and the production of hydroxyls is energetically downhill. S sites common to Fe-OH and Fe-O groups (i.e., HO-Fe-S-Fe-O linkages) are also partially electron depleted. Nucleophilic attack by available surface hydroxyls at these sites would lead to S-O groups in a way that is consistent with the known overall oxidation mechanism on the basis of isotopic oxygen tracer studies (e.g., Reedy et al., 1991).

4. IMPLICATIONS OF THE PROXIMITY EFFECT

As described in this report, electronic structure calculations for galena strongly suggest that because of the delocalized nature of electrons in semiconductors, a species interacting with a semiconducting surface site can influence another site some distance away through electron transfer. We also show explicitly with STM and STS for pyrite that the reaction of one site influences the electronic structure, and therefore the reactivity of neighboring sites. This means that with the help of spectroscopic and quantum mechanical methods, it is possible to derive the mechanism by which the electronic structure of the near surface layers is modified to influence mutually the reactivity of two or more different types of reactants that are some distance apart from each other. Therefore, this approach may be complementary to complexation models—e.g., the constant capacitance, double- or triple-layer models (Davis and Kent, 1990) or the CD MUSIC model (Hiemstra and Van Riemsdijk, 1999), the often successful and useful models long used to rationalize macroscopic observations of the sorption/desorption of aqueous species to/from mineral surfaces. It has to be noted that it is often not possible, or only indirectly possible, to resolve interaction mechanisms from fitting adsorption isotherms such as the FFG isotherm to experimental data (Stumm, 1992; Junta et al., 1995). On the other hand, deriving adsorption isotherms exclusively from the methods presented in this article would be hard and not very precise, especially when the isotherms are evaluated as a function of other environmental parameters (pH, ionic strength, temperature, etc.).

One influence that would be desirable to take into account more is the role of water. Incorporation of a hydration sphere around the cluster into the model would, to a minor degree, change the local electronic properties of the PbS cluster and the adsorbed species. Such a hydration sphere could influence more significantly the mobilization and the path of the hydroxide ion. However, by introducing one or more static layers of water into the quantum mechanical model, the error in fixing adsorbed species with static H_2O molecules may be bigger than in the vacuum model presented in this study. A possible solution (a full quantum mechanical molecular dynamics simulation of the cluster with, e.g., two water layers around it—a formidable task at this point, and one beyond the scope of this article) is to indicate possible reaction mechanisms.

Because of the strengths and shortcomings of the separate microscopic and macroscopic approaches, it is necessary to apply both. The spectroscopic/quantum mechanical approach provides an impression of possible mechanisms and aids in choosing a surface complexation model, and the complexation model provides macroscopic quantification.

It will be a challenging task in the future to derive a concise theory for surface complexation that will include most of the parameters inherent to the phenomena described in this study. First and most easily, there is the concentration of the two (or more) reactants that interact via the surface. Next, there is the question over what distance two reactants can interact or how the interaction decreases with distance. This parameter would be a function of the conductivity of the mineral—or, to be more precise, of the width of the band gap at the semiconducting mineral surface, the charge carrier concentration, and the mobility of these charge carriers in the near surface region of the mineral. Becker et al. (1997b) have shown that tens of surface and near surface S atoms can contribute partial charges to a gold complex adsorbed to a PbS surface, leading to the subsequent reduction of the adsorbed gold species. From this, we learn how far-reaching this mechanism can be, often much further than what we can calculate (in terms of cluster size or surface unit cell size) at this time at a quantum mechanical level. Thus, the gold reduction reaction may be enhanced or hindered by another species that is adsorbed tens of ångstroms away.

There are many examples where reactions may be driven by previously unrecognized proximity effects, including both geologically important reactions as well as technical ones. One such example is the Mn adsorption/oxidation on hematite surfaces. Junta and Hochella (1994) found that this process is accelerated on hematite relative to goethite and it is dramatically faster than on albite surfaces. In addition, the process is highly promoted on hematite steps as compared with terraces. That means that the hematite surface steps promote the electron transfer from the manganese to the oxygen. It is interesting to note that the difference in the bulk band gap between hematite and goethite is small and therefore is not a good explanation for differences in the reactivity. However, the band gap of the hematite surface is much smaller than for the bulk, and the density of states near the Fermi level at steps is highly increased (Becker et al., 1996). Therefore, it can be speculated that these kinds of reactions are mainly influenced by the characteristics of the electronic structure of steps, and proximity effects could be expected to take place predominantly at steps. Thus, in terms of the model depicted in Figure 2, the main path of charge and spin density transfer may not be perpendicular to the steps through the near surface region but rather along the steps.

Another important reaction type where proximity effects may play an important role are, e.g., redox reactions involving arsenic on mineral surfaces. Arsenic mobilization from aquatic sediments is an environmental problem because waterborne arsenic can migrate into pristine areas, endangering aquatic organisms and people (Ahmann et al., 1997). In this respect, it is important to know what the redox mechanisms are that transform arsenic from one oxidation state to another because

these redox processes often control the mobility of this hazardous element. Nesbitt and Reinke (1999) found that the initiation of arsenic oxidation on niccolite (NiAs) may involve the reduction of adsorbed atomic oxygen radicals and the production of $As(OH)_3$ surface species. In light of the proposed proximity effect, one has to ask where the oxygen radicals adsorb on the surface with respect to the sites where the formation of surface (oxy-)hydroxide species occurs. Thus, charge transfer of electrons from atomic O atoms through the NiAs to the oxidized As that gets hydrated is a likely mechanism. Another level of complexity is added if bacteria are involved as the electron donating species. One example for such a multistep charge transfer through or along surfaces is when the dissimilatory Fe(III)-reducing bacterium *Shewanella alga*BrY provides the electron for the reduction of Fe(III) to Fe(II) in As containing Fe (oxy-)hydroxides. Subsequently, the electron can be transferred to reduce As(V), and arsenic is released from the surface to solution (Cummings et al. 1999, 2000).

Our last example deals with multicomponent redox reactions in collectorless flotation. Kartio et al. (1998) describe redox reactions of Cu and Zn on sphalerite surfaces as a function of oxygen in solution (and thus oxygen adsorbed to the surface). These reactions are important when Cu from solution is used in the form of CuS-like adsorbates for the flotation activation of ZnS. In the absence of oxygen, Cu(II) is reduced at the surface, whereas the sulfur in ZnS gets oxidized. When oxygen is present, electron transfer chooses a different path and results in the formation Cu-polysulfides that are detrimental to the activation process. In this example, it would be important to know to what degree these reactions are dependent on, e.g., the iron content of the sphalerite. We know that this class of reactions is very dependent on the semiconducting properties of the reactive substrate, and we know that sphalerite only becomes conductive at high contents of foreign cations. Thus, the complicated electron transfer mechanisms described above would be enhanced for sphalerite with a high degree of impurities such as Fe (electrons can be transferred over longer distances) or at high concentrations of the reactants at the surface that makes next-neighbor interactions more likely.

These are only some of many examples in which semiconducting sulfide and oxide surfaces where electron transfer between two or more reacting species may take place over some distance. Thus, there is a whole class of reactions that can occur on semiconducting surfaces that may be better understood in the future if the influence of surface species and bulk admixtures on the band structure of the substrate are known. These surfaces may be of geologic origin, or they may be on semiconductors that may be of interest to engineers or physicists.

Acknowledgments—We thank Don Rimstidt and Jerry Gibbs (Virginia Tech) for discussions. This study was funded by two grants from the National Science Foundation (EAR 96-9628023 and EAR 99-9902996), by the Habilitationsstipendium (1952/1-3) from the Deutsche Forschungsgemeinschaft, and by the Office of Basic Energy Science, Geosciences Program, U.S. Department of Energy (DOE). Pacific Northwest National Laboratory is operated for the DOE by Battelle Memorial Institute under contract DE-AC06-76RLO 1830.

Associate editor: D. L. Sparks

REFERENCES

Ahmann D., Krumholz L. R., Hemond H. F., Lovley D. R., and Morel F. M. M. (1997) Microbial mobilization of arsenic from sediments of the Aberjona Watershed. *Environ. Sci. Technol.* **31,** 2923–2930.

Albery W. J., Oshea G. J., and Smith A. L. (1996) Interpretation and use of Mott-Schottky plots at the semiconductor/electrolyte interface. *J. Chem. Soc. Faraday Trans.* **92,** 4083–4085.

Ardizzone S., Hoiland H., Lagioni C., and Sivieri E. (1998) Pyridine and aniline adsorption from an apolar solvent: The role of the solid adsorbent. *J. Electroanalyt. Chem.* **447,** 17–23.

Barrow N. J. (1987) *Reactions with Variable Charge Soils.* Martinus Nijhoff.

Becker U. and Hochella M. F. Jr. (1996) The calculation of STM images, STS spectra, and XPS peak shifts for galena: New tools for understanding mineral surface chemistry. *Geochim. Cosmochim. Acta* **60,** 2413–2426.

Becker U., Hochella M. F. Jr., and Aprà E. (1996) The electronic structure of hematite (001) surfaces: Applications to the interpretation of STM images and heterogeneous surface reactions. *Am. Mineral.* **81,** 1301–1313.

Becker U., Munz A. W., Lennie A. R., Thornton G., and Vaughan D. J. (1997a) The atomic and electronic structure of the (001) surface of monoclinic pyrrhotite (Fe_7S_8) as studied by using STM, LEED, and quantum mechanical calculations. *Surface Sci.* **389,** 66–87.

Becker U., Vaughan D. J., and Hochella M. F. Jr. (1997b) The adsorption of gold to galena surfaces: Calculation of adsorption/reduction energies, reaction mechanisms, XPS spectra, and STM images. *Geochim. Cosmochim. Acta* **61,** 3565–3585.

Becker U., Greatbanks S. P., Rosso K. M., Hillier I. H., Vaughan D. J. (1997c) An embedding approach for the calculation of STM images: Method development and application to galena (PbS) *J. Chem. Phys.* **107,** 7537–7542.

Bosbach D., Hall C., and Putnis A. (1998) Mineral precipitation and dissolution in aqueous solution: In situ microscopic observations on barite (001) with atomic force microscopy. *Chem. Geol.* **151,** 143–160.

Buckley A. N. and Woods R. (1984) An x-ray photoelectron spectroscopic study of the oxidation of galena. *Appl. Surface Sci.* **17,** 401–414.

Cisneros-Gonzalez I., Oropeza-Guzman M. T., and Gonzalez I. (1999) Cyclic voltammetry applied to the characterisation of galena. *Hydrometallurgy* **53,** 133–144.

Cornell R. M. and Schwertmann U. (1996) *The Iron Oxides.*VCH.

Cummings D. E., Caccavo F., Fendorf S., and Rosenzweig R. F. (1999) Arsenic mobilization by the dissimilatory Fe(III)-reducing bacterium *Shewanella alga*BrY. *Environ. Sci. Technol.* **33** 723–729.

Cummings D. E., March A. W., Bostick B., Spring S., Caccavo F., Fendorf S., and Rosenzweig R. F. (2000) Evidence for microbial Fe(III) reduction in anoxic, mining-impacted lake sediments (Lake Coeur d'Alene, Idaho). *Appl. Environ. Microbiol.* **66,** 154–162.

Davis J. A., and Kent D. B. (1990) Surface complexation modeling in aqueous geochemistry. In *Mineral–Water Interface Geochemistry* (eds. M. F. Hochella and A. F. White), pp. 177–248. Mineralogical Society of America.

Drever J. I. and Stillings L. L. (1997) The role of organic acids in mineral weathering. *Colloids Surfaces A Physicochem. Eng. Aspects* **120,** 167–181.

Dzombak D. A. and Morel F. M. M. (1990) *Surface Complexation Modeling: Hydrous Ferric Oxide.*Wiley.

Eggleston C. M. (1999) The surface structure of α-Fe_2O_3 (001) by scanning tunneling microscopy: Implications for interfacial electron transfer reactions. *Am. Mineral.* **84** 1061–1070.

Eggleston C. M., Ehrhardt J. J., and Stumm W. (1996) Surface structural controls on pyrite oxidation kinetics: An XPS-UPS, STM, and modeling study. *Am. Mineral.* **81,** 1036–1056.

Ellmer K. and Hopfner C. (1997) On the stoichiometry of the semiconductor pyrite (FeS_2). *Philosophical Magazine A: Physics of Condensed Matter Structure. Defects and Mechanical Properties* **75,** 1129–1151.

Fohlisch A., Nyberg M., Bennich P., Triguero L., Hasselstrom J., Karis O., Pettersson L. G. M., and Nilsson A. (2000) The bonding of CO to metal surfaces. *J. Chem. Phys.* **112,** 1946–1958.

Frisch M. J., Trucks G. W., Schlegel H. B., Scuseria G. E., Robb M. A., Cheeseman J. R., Zakrzewski V. G., Montgomery J. A. Jr., Stratmann R. E., Burant J. C., Dapprich S., Millam J. M., Daniels A. D., Kudin K. N., Strain M. C., Farkas O., Tomasi J., Barone V., Cossi M., Cammi R., Mennucci B., Pomelli C., Adamo C., Clifford S.,

Ochterski J., Petersson G. A., Ayala P. Y., Cui Q., Morokuma K., Malick D. K., Rabuck A. D., Raghavachari K., Foresman J. B., Cioslowski J., Ortiz J. V., Baboul A. G., Stefanov B. B., Liu G., Liashenko A., Piskorz P., Komaromi I., Gomperts R., Martin R. L., Fox D. J., Keith T., Al-Laham M. A., Peng C. Y., Nanayakkara A., Gonzalez C., Challacombe M., Gill P. M. W., Johnson B., Chen W., Wong M. W., Andres J. L., Gonzalez C., Head-Gordon M., Replogle E. S., and Pople J. A. (1998) Gaussian 98, revision A.7. Gaussian Inc.

Gokhale S., Trischberger P., Menzel D., Widdra W., Droge H., Steinruck H. P., Birkenheuer U., Gutdeutsch U., and Rosch N. (1998) Electronic structure of benzene adsorbed on single-domain Si(001)-(2×1): A combined experimental and theoretical study. *J. Chem. Phys.* **108,** 5554–5564.

Guevremont J. M., Elsetinow A. R., Strongin D. R., Bebie J., and Schoonen M. A. A. (1998) Structure sensitivity of pyrite oxidation: Comparison of the (100) and (111) planes. *Am. Mineral.* **83,** 1353–1356.

Hamers R. J., Chen X., Frank E. R., Higgins S. R., Shan J., and Wang Y. (1996) Atomically-resolved investigations of surface reaction chemistry by scanning tunneling microscopy. *Isr. J. Chem.* **36,** 11–24.

Herrmann J. M. and Disdier J. (2000) Electrical properties of V_2O_5-WO_3/TiO_2 EUROCAT catalysts, evidence for redox process in selective catalytic reduction (SCR) deNO(x) reaction. *Catalysis Today* **56,** 389–401.

Hiemstra T. and Van Riemsdijk W. H. (1999) Surface structural ion adsorption modeling of competitive binding of oxyanions by metal (hydr)oxides. *J. Colloid Interface Sci.* **210,** 182–193.

Higgins S. R. and Hamers R. J. (1996) Chemical dissolution of the galena(001) surface observed using electrochemical scanning tunneling microscopy. *Geochim. Cosmochim. Acta* **60,** 3067–3073.

Hingston F. J. (1981) A review of anion adsorption. In *Adsorption of Inorganics at Solid-Liquid Interfaces* (eds. M. A. Anderson and A. J. Rubin), pp. 51–90, Ann Arbor Science Publications.

Jambor J. L. and Blowes D. W. (eds.) (1994) *Short Course Handbook on Environmental Geochemistry of Sulfide Mine-Wastes.* Mineralogical Association of Canada.

James R. O. and Parks G. A. (1982) Characterization of aqueous colloids by their electrical double layer and intrinsic surface chemical properties. In *Surface and Colloid Science*, Vol. 12, chap. 2, pp. 119–216, Plenum Press.

Junta J. and Hochella M. F. (1994) Manganese(II) oxidation at mineral surfaces—A microscopic and spectroscopic study. *Geochim. Cosmochim. Acta* **58,** 4985–4999.

Junta J. L., Hochella M. F. Jr., and Rimstidt J. D. (1995) The dangers of justifying sorption mechanisms with solution data—Mn(II) adsorption oxidation precipitation. GEOC Part 1. *Abstr. Pap. Am. Chem. Soc.* **209,** 69.

Kartio I. J., Basilio C. I., and Yoon R. H. (1998) An XPS study of sphalerite activation by copper. *Langmuir* **14,** 5274–5278.

Kim B. S., Hayes R. A., Prestidge C. A., Ralston J., and Smart R. St. C. (1994) Scanning tunnelling microscopy studies of galena: The mechanism of oxidation in air. *Appl. Surface Sci.* **78,** 385–397.

Koretsky C. M., Sverjensky D. A., and Sahai N. (1998) A model of surface site types on oxide and silicate minerals based on crystal chemistry: Implications for site types and densities, multi-site adsorption, surface infrared spectroscopy, and dissolution kinetics. *Am. J. Sci.* **298,** 349–438.

Kraepiel A. M. L., Keller K., and Morel F. M. M. (1999) A model for metal adsorption on montmorillonite. *J. Colloid Interface Sci.* **210,** 43–54.

Kubota N., Yokota M., and Mullin J. W. (2000) The combined influence of supersaturation and impurity concentration on crystal growth. *J. Crystal Growth* **212,** 480–488.

Lin H. K. and Say W. C. (1999) Study of pyrite oxidation by cyclic voltammetric, impedance spectroscopic and potential step techniques. *J. Appl. Electrochem.* **29,** 987–994.

Maldonado-Hodar F. J., Madeira L. M., Portela M. F., Martin-Aranda R. M., and Freire F. (1996) Oxidative dehydrogenation of butane: Changes in chemical, structural and catalytic behavior of Cs-doped nickel molybdate. *J. Mol. Catalysis A Chem.* **111,** 313–323.

Montes S., Valero E., and Schmidt Y. R. (2000) Study of the flotation mechanisms of quartz in the presence of alkylammonium salts. I. Effect of pH value. *Bol. Soc. Chilena Quimica* **45,** 31–39.

Moore W. J. and Pauling L. (1941) The crystal structure of the tetragonal monoxides of lead, tin, palladium and platinum. *J. Am. Chem. Soc.* **63,** 1392–1394.

Müller P., Kern R., Ranguis K. A., and Zerwetz, G. (1994) Adsorption-isotherms of Ag/Si(111)7×7. *Europhy Lett.* **26,** 461–466.

Murray P. W., Leibsle F. M., Muryn C. A., Fisher H. J., Flipse C. F. J., and Thornton G. (1994) Extended defects on TiO_2 (100) 1 53 3. *Surface Sci.* **321,** 217–228.

Natarajan A., Oskam G., and Searson P. C. (1998) The potential distribution at the semiconductor/solution interface. *J. Phys. Chem. B* **1102,** 7793–7799.

Nesbitt H. W. and Reinke M. (1999) Properties of As and S at NiAs, NiS, and $Fe_{1-x}S$ surfaces, and reactivity of niccolite in air and water. *Am Mineral.* **84,** 639–649.

Nilsson A., Wassdahl N., Weinelt M., Karis O., Wiell T., Bennich P., Hasselstrom J., Fohlisch A., Stohr J., and Samant M. (1997) Local probing of the surface chemical bond using X-ray emission spectroscopy. *Appl. Physics A Mater. Sci. Proc.* **65,** 147–154.

Oertel J., Ellmer K., Bohne W., Rohrich J., and Tributsch H. (1999) Growth of n-type polycrystalline pyrite (FeS_2) films by metalorganic chemical vapour deposition and their electrical characterization. *J. Crystal Growth* **199,** 1205–1210.

Pascual J. I., Gomez-Herrero J., Rogero C., Baro A. M., Sanchez-Portal D., Artacho E, Ordejon P., and Soler J. M. (2000) Seeing molecular orbitals. *Chem. Physics Lett.* **321,** 78–82.

Pettenkofer C., Jaegermann W., and Bronold M. (1991) Site specific surface interaction of electron-donors and acceptors on FeS_2(100) cleavage planes. *Ber. Bunsen-Gesellschaft-Phys. Chem. Chem. Physics* **95,** 560–565.

Pina C. M., Becker U., Risthaus P., Bosbach D., and Putnis A. (1998) Molecular-scale mechanisms of crystal growth in barite. *Nature* **395,** 483–486.

Poulson S. R., Drever J. I., and Stillings L. L. (1997) Aqueous Si-oxalate complexing, oxalate adsorption onto quartz, and the effect of oxalate upon quartz dissolution rates. *Chem. Geol.* **140,** 1–7.

Prestidge C. A., Ralston J., and Smart R. S. (1993) The role of cyanide in the interaction of ethyl xanthate with galena. *Colloids Surfaces A Physicochem. Eng. Aspects* **81,** 103–119.

Reedy B. J., Beattie J. K., and Lowson R. T. (1991) A vibrational spectroscopic ^{18}O tracer study of pyrite oxidation. *Geochim. Cosmochim. Acta* **55,** 1609–1614.

Rimstidt J. D., Chermak J. A., and Gagen, P. M. (1994) Rates of reaction of galena, sphalerite, chalcopyrite, and arsenopyrite with Fe(III) in acidic solutions. In *Environmental Geochemistry of Sulfide Oxidation* (eds. C. N. Alpers and D. W. Blowes), pp. 2–13. American Chemical Society.

Rosso K. M. and Hochella M. F. Jr. (1999) A UHV STM/STS and *ab initio* investigation of covellite (001) surfaces. *Surface Sci.* **423,** 364–374.

Rosso K. M., Becker U., and Hochella M. F. Jr. (1999a) Atomically resolved electronic structure of pyrite (100) surfaces: An experimental and theoretical investigation with implications for reactivity. *Am. Mineral.* **84,** 1535–1548.

Rosso K. M., Becker U., and Hochella M. F. Jr. (1999b) The oxidation of pyrite (100) surfaces with O_2 and H_2O: Fundamental oxidation mechanisms. *Am. Mineral.* **84,** 1549–1561.

Rufe E. and Hochella M. F. Jr. (1999) Quantitative assessment of reactive surface area of phlogopite during acid dissolution. *Science* **285,** 874–876.

Srinivasan K., Meera K., and Ramasamy P. (2000) A novel method to enhance metastable zone width for crystal growth from solution. *Crystal Res. Technol.* **35,** 291–297.

Stumm W. (1992) *Chemistry of the Solid–Water Interface.* Wiley.

Suganuma Y. and Tomitori M. (2000) Analysis of electron standing waves in a vacuum gap of scanning tunneling microscopy: Measurement of band bending through energy shifts of electron standing wave. *J. Vacuum Sci. Technol. B* **18,** 48–54.

Svensson U. and Dreybrodt W. (1992) Dissolution kinetics of natural calcite minerals in CO_2-water systems approaching calcite equilibrium. *Chem. Geol.* **100,** 129–145.

Tao D. P., Li Y. Q., Richardson P. E., and Yoon R. H. (1994) The incipient oxidation of pyrite. *Colloids Surfaces A Physicochem. Eng. Aspects* **93,** 229–239.

Tessis A. C., Penteado-Fava A., Pontes-Buarque M., De Amorim H. S., Bonaface J. A. P., De Souza-Barros F., and Vieyra A. (1999) Pyrite suspended in artificial sea water catalyzes hydrolysis of adsorbed ATP: Enhancing effect of acetate. *Origins Life Evol. Biosphere* **29,** 547–547.